

## WAVES BEHIND A STEP IN AN OPEN CHANNEL

V. I. Bukreev and A. V. Gusev

UDC 532.59

*The paper presents experimental data on flow in the vicinity of a sudden elevation of channel bottom (step). The range of external flow parameters is considered for the case where the step generates waves. A distinguishing feature of these waves is that they are formed in transition from subcritical to supercritical flow. It is shown that there is a range of external parameters in which the depth at the channel exit, the depth above the step, and the distance from the step to the first wave trough depend exclusively on flow discharge.*

**Key words:** *experiment, open channel, uneven bottom, wave profiles, critical depths.*

**Introduction.** In recent years, considerable attention has been given to water ecological problems, in particular, to calculations of extreme natural processes in open channels and consequences of accidental failures of hydraulic constructions. Yet, the mathematical models employed in such calculations are not realistic. For example, for the problem of dam break, valuable results were obtained by calculations using Saint Venant's equations [1, 2]. However, because these equations employ hydrostatic pressure distribution over depth, they do not adequately describe waves such as undular bores, formed during the evolution of rather intense disturbances [3, 4]. This stimulates the development of more adequate models and derivation of experimental data for their testing.

The most promising trends in improving mathematical models involve considering the nonhydrostaticity of pressure distribution over flow depth, mixing processes, and vorticity [5–7]. Of special interest for testing such models are experimental data on flows in which nonhydrostaticity, mixing, and strong vorticity are clearly manifested in steady-state regimes. This is the case, for example, in steady flow in the vicinity of a step, a drop, or a sill on the channel bottom. Here the term “step” denotes a sudden downstream rise of the channel bottom and the term “drop” denotes sudden lowering of the channel bottom. A combination of a step and a drop is called a “sill” if the step precedes the drop, and it is called a “trench” if the drop is ahead of the step. The term “barrier” denotes a smooth rise of a bottom with a subsequent smooth lowering [7, 8].

The present paper deals with an experimental study of flow past a step. This flow is of interest for testing mathematical models because the effect of nonhydrostaticity and vorticity is manifested under steady conditions. As shown below, the regularities involved in this flow can be used to construct closure relations in mathematical models. In addition, undular bore type waves exist behind a step under certain conditions, but, unlike undular bores, they are formed in subcritical flow. The same waves can be generated by the upstream edge of a rectangular sill [5, 9]. More complete information on flow over a rectangular sill is given in [10, 11]. Flow behind a drop has been studied experimentally, for example, in [12]. Data on flows over streamlined obstacles are reviewed in [8]. We note that in the case of flow over a streamlined obstacle, the waves considered in the present paper do not exist because they are generated mainly by flow separation from a step or the upstream edge of a sill.

**1. Experimental Procedure.** The experiments were performed in rectangular channel of width  $B = 6$  cm. The bottom slope was zero ahead of and behind the step. At the channel exit, the flow discharged freely into the atmosphere. A step of height  $b$  was a distance  $l$  upstream of the channel exit. Eight runs of experiments were performed for different  $b$  and/or  $l$  (Table 1). In run No. 1, we studied a flow in the channel without a step. In each run, we set 10–12 values of the volumetric discharge  $Q$  in the range from 0.3 to 4.4 liters/sec. For  $Q$  close to the lower limit of this range, the discharge was measured by a volumetric method. For volumetric discharge exceeding

---

Lavrent'ev Institute of Hydrodynamics, Siberian Division, Russian Academy of Sciences, Novosibirsk 630090. Translated from *Prikladnaya Mekhanika i Tekhnicheskaya Fizika*, Vol. 44, No. 1, pp. 62–70, January–February, 2003. Original article submitted April 18, 2002; revision submitted July 23, 2002.

TABLE 1

Run number	$b$ , cm	$l$ , cm	Run number	$b$ , cm	$l$ , cm
1	0	—	5	4.85	30
2	2.45	30	6	4.85	60
3	2,45	60	7	4.85	123
4	2.45	123	8	2.40	15

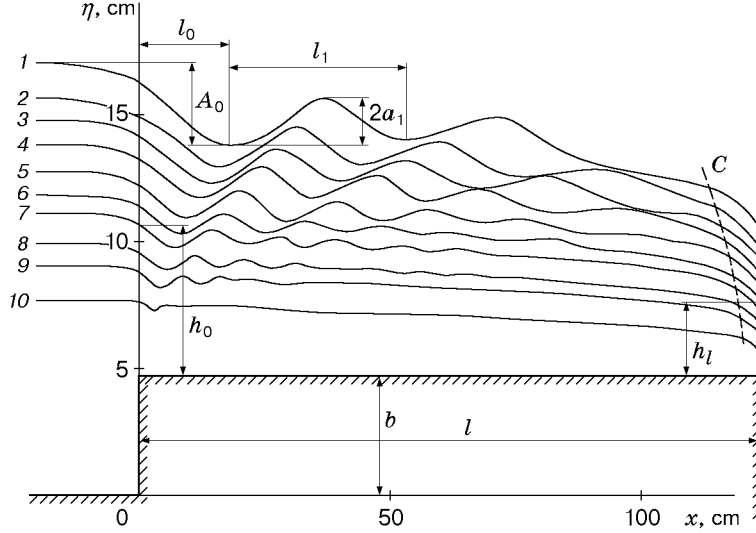


Fig. 1. Wave profiles for  $b = 4.85$  cm,  $l = 123$  cm, and  $h_* = 7.45$  (1), 6.61 (2), 6.35 (3), 6.0 (4), 4.64 (5), 4.03 (6), 3.50 (7), 2.78 (8), 2.28 (9), and 1.45 (10): the dashed curve corresponds to  $\eta - b = h_*$ .

0.8 liters/sec, high accuracy was provided for by a standard Venturi tube calibrated previously by a volumetric method. The measurement error for  $Q$  did not exceed 1%.

The main measured parameter was the free-surface profile  $\eta(x, \Pi_i)$  ( $\eta$  is the vertical coordinate of the free surface reckoned from the channel bottom ahead of the step,  $x$  is the longitudinal coordinate reckoned downstream from the step, and  $\Pi_i$  is the set of problem parameters). The profile was measured with a measuring needle (absolute error less than  $\pm 0.5$  mm). For visualization of the internal flow structure, in particular in the region of flow separation from the step, aluminum particles were introduced into the flow.

The set of problem parameters  $\Pi_i$  includes the parameters  $B$ ,  $b$ ,  $l$ , and  $Q$ , the acceleration of gravity  $g$ , the kinematic viscosity coefficient  $\nu$ , and the roughness of the wall channels  $\Delta$ . Since the fluid was homogeneous and incompressible and we studied only kinematic flow characteristics, the fluid density was not included in the number of parameters. In these experiments, the capillary effects were negligible. However, in some cases, for example, for wave breakup, this set of parameters should include the surface tension coefficient  $\sigma$ . The parameters  $B$ ,  $g$ ,  $\nu$ , and  $\Delta$  were constant in the experiments. The channel walls and bottom were made of Plexiglas. Tap water at a temperature of 12–14°C was used.

In hydraulics, the quantities  $B$ ,  $Q$ , and  $g$  form the characteristic linear dimension [10, 11]

$$h_* = (q^2/g)^{1/3} \quad (q = Q/B),$$

which is called the critical depth. The external parameter  $h_*$  can be considered an equivalent of  $Q$ . When this parameter is used, many dimensional parameters varied in the experiments reduce to the three independent linear dimensions:  $h_*$ ,  $b$ , and  $l$ . In the present paper, we consider only subcritical flow of depth  $h_{-\infty} > h_*$  coming over the step. The case of supercritical step overflow requires a separate study. Below, along with  $h_*$ , we consider another critical depth  $h_{**} < h_*$ . Therefore,  $h_*$  is called the first critical depth and  $h_{**}$  the second critical depth.

To analyze results of the measurements, we considered several characteristic values of the function  $\eta(x, \Pi_i)$ : the depth  $h_0 = \eta(0) - b$  immediately above the step, the depth  $h_l = \eta(l) - b$  at the channel exit, the characteristic wave amplitude, and the characteristic wavelength (Fig. 1). The amplitude was determined as half the vertical distance between a wave trough and the downstream neighboring wave crest. The lengths of waves with uneven numbers were found as the horizontal distance between neighboring troughs, and the lengths of waves with even

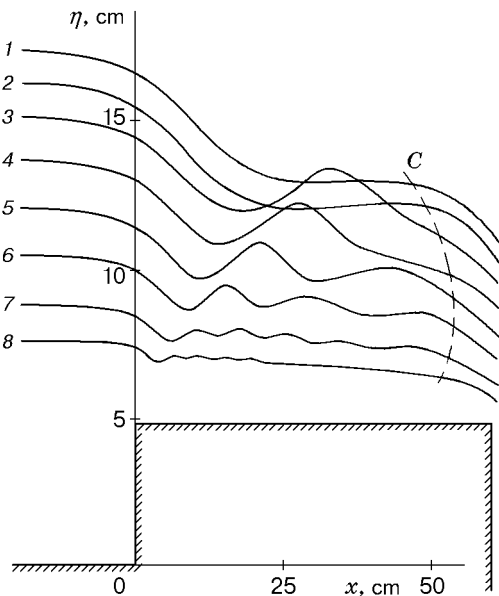


Fig. 2

Fig. 2. Free-surface profiles for  $b = 4.85$  cm,  $l = 60$  cm, and  $h_* = 8.10$  (1), 7.32 (2), 6.43 (3), 5.40 (4), 4.28 (5), 3.25 (6), 2.24 (7), and 1.57 (8): the dashed curve corresponds to  $\eta - b = h_*$ .

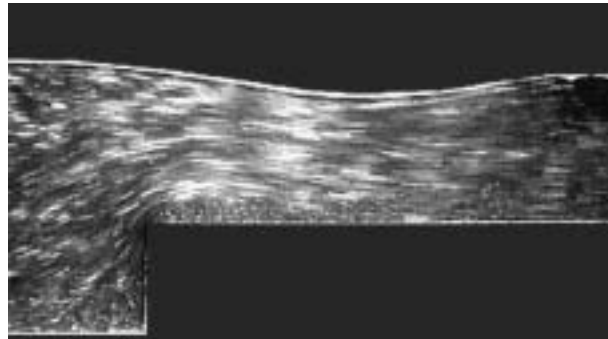


Fig. 3

Fig. 3. Internal flow structure in the vicinity of the step ( $b = 4.85$  cm,  $l = 30$  cm, and  $h_* = 8.5$  cm).

numbers were found as the distance between neighboring crests. The depth of the first trough  $A_0$  and the distance from this trough to the step  $l_0$  were calculated separately.

We compared various methods for choosing characteristic scales for conversion to dimensionless variables. It was established that some regularities are manifested more clearly if dimensional rather than dimensionless quantities are used in analysis. For example, some sought quantities depended only on  $h_*$  and did not depend on  $b$  and  $l$ . In this case, conversion to dimensionless variables led to loss of this universal dependence. Therefore, below all experimental data are given in dimensional form.

**2. Experimental Results.** Figures 1 and 2 show examples of free-surface profiles (the dashed curves  $C$  correspond to critical depths; on the right of these depths, the flow is subcritical and on the left, the flow is supercritical). Our experiments yielded a very interesting result: in all experiment runs, the waves behind the step exist only in subcritical flow (see Figs. 1 and 2). Undular bore waves formed in transition from supercritical to subcritical flow have been adequately studied [4, 5, 11, 12]. In the case of flow over a rectangular sill, waves can exist in both subcritical and supercritical flows because, in this case, they are generated by both the upstream and downstream edges of the sill [9].

An important condition for the existence of waves in subcritical flow is flow separation from the step. Figure 3 shows a photograph of the internal flow structure in the vicinity of a step for the case of wave formation. A stagnation zone with one large and several small vortices is formed ahead of the step; solid particles are rarely transferred from this zone to the outer flow. In the case considered, the vertical dimension of the flow separation zone behind the sharp edge is a significant part of the flow depth. In this case, noticeable waves are formed behind the step. With increase in  $h_*$  and decrease in  $b$  and  $l$ , the wave amplitudes tend to zero.

Some free-surface profiles observed in our experiments are shown schematically in Fig. 4. Here the values of  $h_*$  and  $h_{**} \approx h_*/1.33$  are also given. The physical meaning of  $h_{**}$  is discussed below. The profile in Fig. 4a corresponds to flow without a step. In this case, a decay curve is formed because of friction on the rigid walls [10, 11]. For a small step height and low discharges ( $b \ll l$  and  $h_* \ll l$ ), the decay curve only shows the local lowering of the surface level in the vicinity of the step (see profile 10 in Fig. 1 and profile 8 in Fig. 2).

Setting constant  $h_*$  and  $b$  and decreasing  $l$ , one observes the sequence of profiles shown in Fig. 4b–e. Waves are formed only in a limited range of parameters (Fig. 4b). The profile shown in Fig. 4c, unlike other profiles, has a horizontal “ledge,” which is formed only for a certain combination of the parameters  $b$ ,  $l$ , and  $h_*$ . The height of

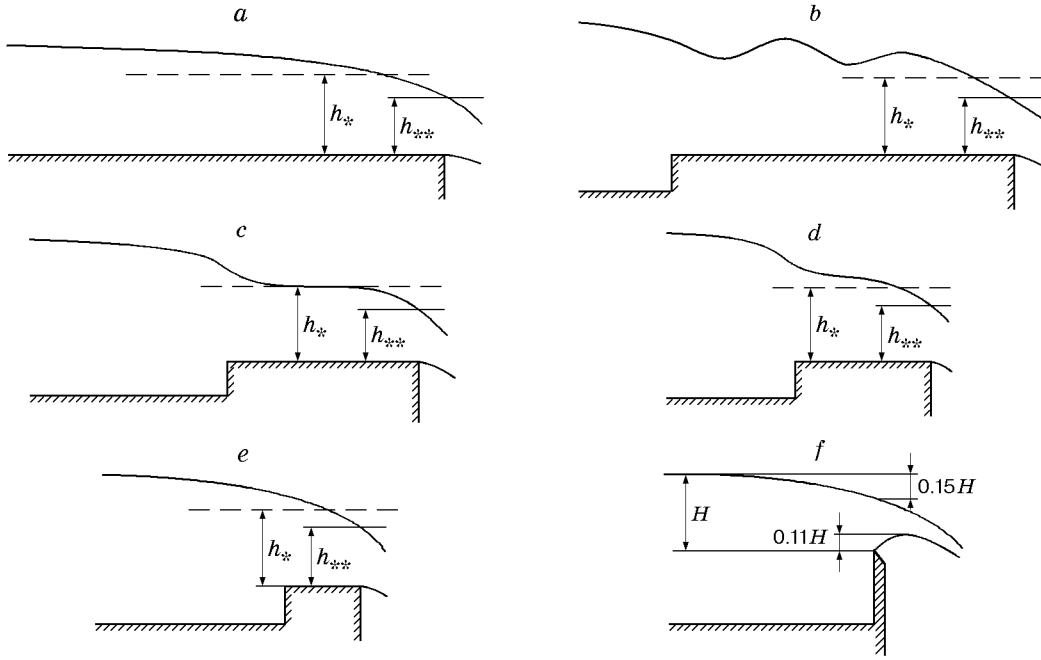


Fig. 4. Possible free-surface profiles behind a step.

this “ledge” above the bottom channel behind the step lies in a small vicinity of  $h_*$ . A further decrease in  $l$  results in regimes with continuously lowering free-surface levels, which have either two (Fig. 4d) or no points (Fig. 4e) of inflection. For comparison, Fig. 4f shows a diagram of flow over a sharp-edged spillway ( $l \rightarrow 0$ ) [10, 11]. In this case, it is important that at the channel exit, the flow is compressed not only from above but also from below. Therefore, in the limit  $l \rightarrow 0$ , the regularities discussed below are disturbed.

Figure 5 shows a curve of depth at the channel exit  $h_l$  versus the critical depth  $h_*$  for all combinations of the parameters  $b$  and  $l$  given in Table 1, including the case of an even bottom. All the experimental data are grouped along the line  $h_l = k_1 h_*$ , where  $k_1 = \text{const}_1 = 0.75 \pm 0.02$ . Therefore, we can state that there is a range of the parameters  $b$  and  $l$  in which the depth at the exit from the channel to the atmosphere depends only on  $h_*$  and this dependence is linear. Of special interest is the value of the proportionality coefficient  $k_1 = 0.75$ , which deserves a more detailed discussion.

The theoretical analysis in [7, 13] and experiments of [4, 13–15] show that for two-dimensional gravity waves on finite depth water there are two characteristic propagation speeds at which the wave picture changes qualitatively. Let us call them the first and second critical speeds [14]. For a homogeneous fluid of depth  $h$  at rest above an even horizontal bottom, the first critical speed is  $c_* = \sqrt{gh}$  and the second critical speed is related to the first critical speed by  $c_{**} \approx 1.3c_*$ . The speed  $c_*$  is the upper boundary of the domain of existence of linear harmonic waves, and the speed  $c_{**}$  is the upper boundary for solitary and cnoidal waves. At propagation speeds exceeding  $c_{**}$ , these nonlinear waves break. The same is true for frequently occurring nonlinear undular bore waves [4, 14, 15]. In a density-stratified fluid, the number of critical speeds is equal to the doubled number of eigenmodes [16].

Physically, the critical speeds in mathematical models reflect the fundamental physical prohibition: the rate of perturbation mass and energy transfer cannot exceed the rate of transfer of information on the perturbation. The first approximation of shallow water theory takes into account only the longitudinal velocity component, and this component is assumed to be constant in the vertical direction. Therefore, this model has only one critical speed  $c_*$ . The second critical speed  $c_{**}$  appears in the second approximation of shallow water theory and in more rigorous models that take into account two velocity components and the nonuniformity of their vertical distribution.

The aforesaid bears a direct relation to the hydraulics of unsteady flows in open channels. From physical considerations, the hydraulics of steady but substantially nonuniform flows should also exhibit two rather than one critical speeds and two corresponding critical depths. The first critical depth is  $h_*$ . The role of this depth in open-channel hydraulics has been extensively studied [10, 11]. This depth corresponds to the first critical speed  $V_* = q/h_*$ . If, by analogy to unsteady flows, the second critical speed in nonuniform steady flow hydraulics is

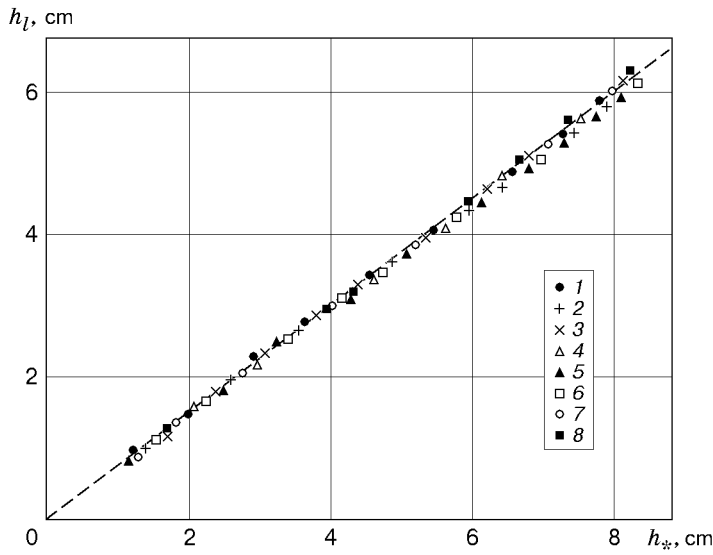


Fig. 5

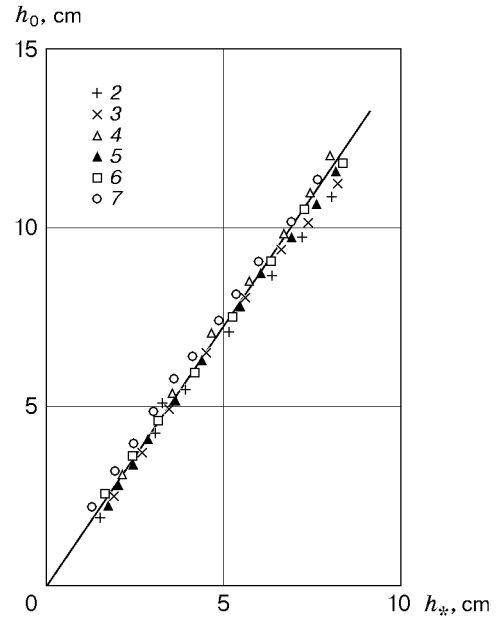


Fig. 6

Fig. 5. Depth at the exit from the channel to the atmosphere versus the first critical depth (experimental point numbers correspond to the run number in Table 1).

Fig. 6. Depth above the step versus the first critical depth (straight line refers to  $h_0 = 1.48h_*$  and the experimental point numbers correspond to the run numbers in Table 1).

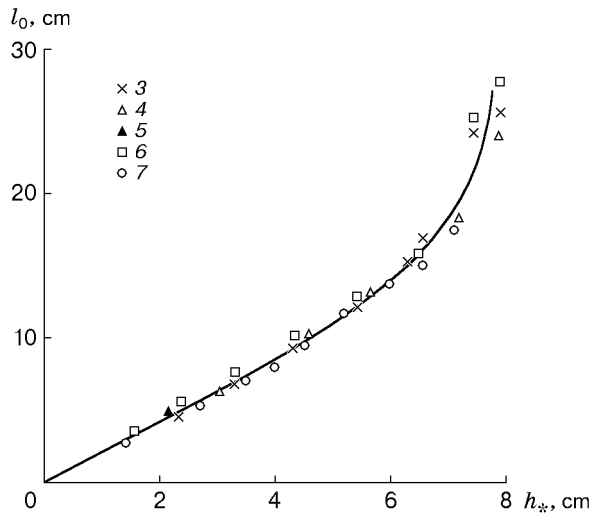


Fig. 7

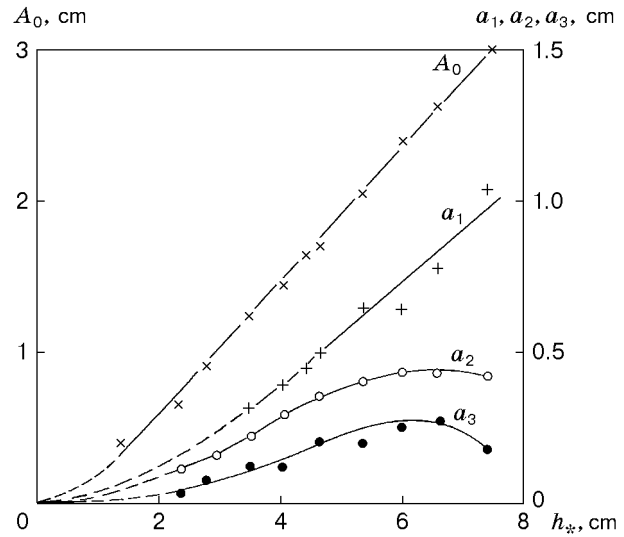


Fig. 8

Fig. 7. Horizontal distance from the step to the first wave trough versus the first critical depth (experimental point numbers correspond to the experiment run numbers in Table 1).

Fig. 8. The depth of the first trough  $A_0$  and wave amplitudes  $a_1$ ,  $a_2$ , and  $a_3$  versus the first critical depth ( $b = 4.85$  cm and  $l = 123$  cm).

TABLE 2

$h_* = 7.45$ cm		$h_* = 6.0$ cm		$h_* = 4.64$ cm		$h_* = 4.03$ cm	
$x$ , cm	$\eta$ , cm	$x$ , cm	$\eta$ , cm	$x$ , cm	$\eta$ , cm	$x$ , cm	$\eta$ , cm
-20	16.95	-20	14.75	-20	12.70	-10	9.85
-15	16.87	-10	14.68	-10	12.70	-5	9.83
-10	16.80	-5	14.50	-5	12.58	-2	9.78
-5	16.60	0	14.00	-2	12.40	0	9.60
0	16.23	3	13.60	0	12.20	2	9.30
4	15.60	6	13.25	3	11.80	5.5	8.95
9	14.70	9	12.75	10	11.00	11.5	9.43
17	13.85	14	12.35	20	12.00	15.5	9.10
24	14.15	21	13.00	29.7	10.90	21	9.30
29	14.70	27	13.65	39.3	11.60	26.3	9.00
36	15.70	33	13.20	48.3	10.95	30.5	9.15
44	14.85	39.5	12.50	57.6	11.35	34.5	9.05
53	14.15	47	13.00	67.7	10.90	39	9.05
62	14.55	52.5	13.30	76.7	11.03	43	9.00
71	15.00	61.5	12.50	90.2	10.48	48.3	9.00
80	14.05	65.5	12.25	100	10.45	52.5	8.90
87	13.50	73	12.35	105.2	10.20	56	8.93
94	13.10	80.5	12.75	112	9.97	61.5	8.80
101	12.75	86	12.40	115	9.83	66	8.85
110	12.50	91	12.00	120	9.03	71	8.74
116	12.10	96	11.60	123	8.40	75.5	8.74
120.3	11.40	103	11.25	—	—	85	8.60
123	10.70	110	11.25	—	—	96	8.40
—	—	113	10.95	—	—	106	8.25
—	—	116	10.60	—	—	116	7.85
—	—	120.3	10.10	—	—	120.3	7.55
—	—	123	9.50	—	—	123	7.00

defined as  $V_{**} = \beta V_*$ , the second critical depth will be defined as  $h_{**} = h_*/\beta$ . Next, if we assume that  $\beta \approx 1.3$ , as in unsteady flow hydraulics, the relation  $h_{**} \approx 0.77h_*$  should hold. The numerical coefficient in this relation differs by only 2.7% from the average experimental value  $k_1 = 0.75$ .

Thus, the experimental data (Fig. 5) show that there is a range of problem parameters in which the depth at the exit from the channel to the atmosphere is equal to the second critical depth. Another case where the second critical depth is manifested in the hydraulics of steady flows is given in [9].

Figure 6 shows experimental data on the depth  $h_0$  immediately above the step. For this quantity, too, there exists a range of the parameters  $b$  and  $l$  in which this quantity depends only on  $h_*$  and this dependence is linear:  $h_0 = k_2 h_*$  ( $k_2 = \text{const}_2$ ). In the experiments, we obtained the value  $k_2 = 1.48 \pm 0.03$ .

In the parameter range considered, the quantity  $l_0$  also does not depend on  $b$  and  $l$  within the measurement error. This is illustrated by the experimental data in Fig. 7 (in experiment run Nos. 1, 2, and 8, waves are absent).

Behind the step  $A_0$ ,  $a_1$ ,  $a_2$ , etc. (see Fig. 1), the wave amplitude characteristics depend in a complex manner on all the parameters of the problem. We only note that there is a range of parameters in which  $A_0$  depends slightly on  $l$ . Figure 8 shows experimental data on the depth of the first trough  $A_0$  and the amplitudes of the first three waves obtained in experiment run No. 6. With increase in  $h_*$  and for fixed  $b$  and  $l$ , these wave parameters first grow, reaching a maximum, and then decrease to zero.

A comparison of the flow considered in the present paper with the flow over a rectangular sill (see, for example, [9]) shows that these flows have both similarities and differences. They differ because in the case of flow behind a sill, the fluid remains in the channel, whereas in the flow considered, it flows freely into the atmosphere. In sill flow, waves can form both ahead of and behind the sill, and these wave systems can interact. In flow over a step, only one wave system is formed. Above the sill, a subcritical incident flow can first enter the supercritical state and then return to the subcritical state. Behind the step, reverse transition from supercritical to subcritical flow was not observed in our experiments. The second critical depth was reached behind the step at the channel exit over a wide range of parameters. In the case of the sill, the second critical depth above the downstream edge of the sill was reached only for a certain combination of parameters, and this was accompanied by significant changes in the internal flow structure [9].

**3. Conclusions.** The fact that the second critical depth is reached at the channel exit (see Fig. 5) is of great importance for mathematical modeling. Owing to this fact, we can use an important closure relation in the system of governing equations. In the case of a sill, the assumption that the first critical depth is reached over the sill plays a similar role [7, 10, 11]. However, this assumption has a limited region of application [9]. In addition, it can be used as an additional closure relation only in mathematical models based on the first approximation of shallow water theory [7]. The experimental results obtained can be used in both the second approximation of shallow water theory and more accurate mathematical models.

The presence of sharp edges of the rigid boundaries of the flow complicates mathematical modeling of the flow. The photograph in Fig. 3 is of interest because it shows a method for solution of this problem by setting a system of concentrated vortices, which ensure the smoothness of streamlines of the main flow. The mathematical models given in [7] can be used in future calculations.

Table 2 lists coordinates of the four characteristic free-surface profiles for  $b = 4.85$  cm and  $l = 123$  cm for quantitative comparison of the numerical calculation results with the experimental data. We thank E. M. Romanova for assistance in derivation of the experimental data and V. A. Kostomakha for help in illustration.

This work was supported by the Russian Foundation for Fundamental Research (Grant No. 01-01-00846), the Foundation for Leading Scientific Schools (Grant No. 00-05-98542), and the Foundation of Integration Programs of the Siberian Division of the Russian Academy of Sciences (Grant No. 1).

## REFERENCES

1. R. E. Dreisler, "Comparison of theories and experiments for the hydraulic dam-break wave," *Int. Assoc. Sci. Hydrology*, No. 38, 319–328 (1954).
2. J. J. Stoker, *Water Waves. The Mathematical Theory with Applications*, Interscience Publishers, New York–London (1957).
3. H. Favre, *Ondes de Translation dans les Canaux Decouverts*, Dunod, Paris (1935).
4. V. I. Bukreev and A. V. Gusev, "Waves ahead of a vertical plate in a channel," *Izv. Ross. Akad. Nauk, Mekh. Zhidk. Gaza*, No. 1, 82–90 (1999).
5. V. V. Smyslov, *Theory of Spillway with a Wide Sill* [in Russian], Izd. Akad. Nauk Ukr. SSR, Kiev (1956).
6. R. K.-C. Chan and R. L. Street, "A computer study of finite amplitude water waves," *J. Comput. Phys.*, **6**, 68–94 (1970).
7. V. Yu. Lyapidevskii and V. M. Teshukov, *Mathematical Models for Propagation of Long Waves in Inhomogeneous Fluids* [in Russian], Izd. Sib. Otd. Ross. Akad. Nauk, Novosibirsk (2000).
8. P. G. Baines, *Topographic Effects in Stratified Flow*, Cambridge Univ. Press, Cambridge (1995).
9. V. I. Bukreev, "Undular jump in open-channel sill overflow," *J. Appl. Mech. Tech. Phys.*, **42**, No. 4, 596–602 (2001).
10. P. G. Kiselyev, *Handbook on Hydraulic Calculations* [in Russian], Gosénergoizdat, Moscow–Leningrad (1957).
11. Ven Te Chow, *Open-Channel Hydraulics*, McGraw Hill Book Co., New York (1959).
12. S. Wu and N. Rajaratnam, "Impinging jet and surface flow regimes at drop," *J. Hydraul. Res.*, **36**, No. 1, 69–74 (1998).
13. L. V. Ovsyannikov, N. I. Makarenko, V. I. Nalimov, et al., *Nonlinear Problems of the Theory of Surface and Internal Waves* [in Russian], Nauka, Novosibirsk (1985).
14. V. I. Bukreev, E. M. Romanov, and N. P. Turanov, "Breaking of gravity waves in a neighborhood of their second critical propagation speed," *J. Appl. Mech. Tech. Phys.*, **39**, No. 2, 205–210 (1998).
15. V. I. Bukreev and V. A. Kostomakha, "Sudden blocking of a subcritical open-channel flow," *J. Appl. Mech. Tech. Phys.*, **42**, No. 1, 35–41 (2001).
16. V. I. Bukreev, "Breaking of gravity waves in the motion of a vertical plate in a two-layer liquid," *J. Appl. Mech. Tech. Phys.*, **39**, No. 5, 659–665 (2001).